Avrupa Bilim ve Teknoloji Dergisi
Özel Sayı 24, S. 47-52, Nisan 2021

Araştırma Makalesi

www.ejosat.com ISSN:2148-2683

European Journal of Science and Technology
Special Issue 24, pp. 47-52, Nisan 2021

Research Article

Bernoulli-Equation-Based Robotic Model for Non-Contact Magnetic Micromanipulation

Jiyan Sürer[1], Ahmet Fatih Tabak[2*]

[1] Kadir Has University, Faculty of Engineering and Natural Sciences, Department of Computer Engineering, Istanbul, Turkey, (ORCID: 0000-0003-3388-7843), 20181701031@stu.khas.edu.tr

[2*] Kadir Has University, Faculty of Engineering and Natural Sciences, Department of Mechatronics Engineering, Istanbul, Turkey, (ORCID: 0000-0003-3311-6942), ahmetfatih.tabak@khas.edu.tr

(2nd International Conference on Access to Recent Advances in Engineering and Digitalization (ARACONF)-10–12 March 2021)

(**DOI:** 10.31590/ejosat.899657)

ATIF/REFERENCE: Sürer J., Tabak, A.F., (2021). Bernoulli-Equation-Based Robotic Model for Non-Contact Magnetic Micromanipulation. *European Journal of Science and Technology*, (24), 47-52.

Abstract

Micromanipulation is an important part of biomedical micro-robotic applications. The lab-on-a-chip applications with live cells and require delicate handling of samples to not compromise their structural integrity. The non-contact micromanipulation via hydrodynamic interactions stands out as an alternative reliable method to avoid this problem. There are several numerical and experimental studies in the literature demonstrating the use of such micro-robotic systems. Furthermore, the analytical models explaining the non-contact manipulation rely on higher-order effects or interfacial interactions along with the inertial forces for rigid-body motion. In this study, the flow field of a free vortex, induced by a rotating magnetic particle, is modeled with the help of conservation of energy across the curvilinear streamlines along with the Magnus effect implicitly implemented in the equation of motion. The streamlines are assumed to be undisturbed although a non-magnetic particle is modeled to be dragged by the induced flow. The rigid body motion of the non-magnetic particle is obtained with the help of drag coefficients and pressure difference along the radial direction. And the pressure difference is predicted along with the rigid-body rotation of the particle along its axis. The results indicate a stable orbit with a constant radial position while the non-magnetic particle completes one full revolution around the core of the free vortex. Furthermore, it has been observed that the step-out phenomenon does not undermine the stability of the rigid-body motion of the particles.

Keywords: non-contact manipulation, robotic simulation, Bernoulli equation, free vortex flow

Temassız Manyetik Mikro Manipülasyon için Bernoulli Denklemine Dayalı Robotik Model

Öz

Mikro manipülasyon, biyomedikal mikro robotik uygulamaların önemli bir parçasıdır. Canlı hücreler ile yapilan testler, yapısal bütünlüklerinden ödün vermemek için numunelerin hassas bir şekilde işlenmesini gerektirir. Hidrodinamik etkileşimler yoluyla temassız mikro manipülasyon, alternatif bir güvenilir yöntem olarak öne çıkmaktadir. Literatürde bu tür mikro robotik sistemlerin kullanımını gösteren çok sayıda sayısal ve deneysel çalışma bulunmaktadır. Ayrıca, temassız manipülasyonu açıklayan analitik modeller, katı cisim hareketi için atalet kuvvetleri ile birlikte yüksek mertebeden etkilere veya arayüzey etkileşimlerine

* Corresponding Author: ahmetfatih.tabak@khas.edu.tr

dayanmaktadır. Bu çalışmada, dönen bir manyetik parçacık tarafından indüklenen zorlanmış bir girdabın akış alanı, hareket denkleminde örtük olarak uygulanan Magnus etkisi ile birlikte akış çizgileri boyunca enerjinin korunumu yardımıyla modellenmiştir. Manyetik olmayan bir partikül, indüklenen akış tarafından sürüklenecek şekilde modellenmesine rağmen, akış çizgilerinin bozulmadığı varsayılmaktadır. Manyetik olmayan parçacığın rijit cisim hareketi, radyal yön boyunca sürükleme katsayıları ve basınç farkı yardımıyla elde edilmektedir. Ve basınç farkı, parçacığın ekseni boyunca katı cisim dönüşü ile birlikte hesaplanmaktadır. Sonuçlar, sabit radyal konuma sahip kararlı bir yörüngeye işaret ederken, manyetik olmayan parçacık, zorlanmış girdabın çekirdeği etrafında bir tam dönüşü tamamlar. Ayrıca, mayetik adım atlama durumunda partiküllerin katı cisim hareketinin stabilitesinin zarar görmediği gözlemlenmiştir.

Anahtar Kelimeler: temassız manipülasyon, robotik simülasyon, Bernoulli denklemi, zorlanmış girdap akışı

1. Introduction

Non-contact manipulation of microparticles, bacteria, and mammalian cells is considered to be one of the promising biomedical applications of the future as the delicate nature of live cells challenges in handling them properly (Zhang et al., 2019). The non-contact approach can be based on magnetics (Diller et al., 2014), optics (Zhang et al., 2020), acoustic waves (Mohanty et al., 2020), and hydrodynamic effects (Diller et al., 2011). The latter is in the focus of this study as, to the best of the author's knowledge, the associated hydrodynamics has not been addressed with an energy-conservation-modeling-approach to incorporate in a definitive robotic model, although there are several studies in the literature addressing the use of a form of hydrodynamic interaction for micromanipulation single or multiple particles.

Ye et al. (2012) investigated the possibility of micromanipulation with rotating flow fields with distant magnetic micro-manipulation and induced rotating fluid. A moving spherical body causes two things due to the various movements of based on rolling and sliding: the rotational fluid flow and the two-dimensional motion of the manipulator. In the force balance, it is concluded that the object's stable orbital attitude in rotational fluids, which are motion criterion and orbital criterion should be met by selection factors. With using these, micro assets can be moved precisely and quickly without any contact. In the interval of the low Re numbers, an object of small sizes can be manipulated accurately. Pieters et al. (2014) investigated the approach to automate the process of protein crystal harvesting via rotating magnetic fields. There is also a visual control system to automatically collect protein crystals, as well as a micro-vehicle and magnetic actuation system. This micro robot is placed in a way that it creates a transverse magnetic field, then it is used to catch and move micro-objects by rolling around the surface on the long axis and forming a vortex. As a result, protein crystals are caught quickly and gently without contact by this approach. Zhang et al. (2019) studied a micro-tool that can take almost all specified shapes and program multiple axes and complex operations. So that; an optoelectronic microrobot, which is described in the article, it used to do manipulation of cells and other living particles. The goal of the approach is a micro-robot controlled by optoelectronic tweezers, and since this micro-robot relies on light to control electrophoresis rather than the force generated by photon momentum, the optoelectronic tweezers perform stronger on manipulation compared to the optical tweezers for a particular photon density. It has also been stated that this process can be used in cell-cell interaction, RNA sequencing and manipulation with a closed system. Floyd et al. (2009) studied the manipulation of underwater microspheres by an electromagnetic micro-robot. The authors present a new method of manipulation: using an unbound magnetic end effector called Mag-µBot, with a micrometers scale. This novel method of manipulation is done in a liquid-immersed environment. This method also finds a numerical solution by reducing the effect of stagnation and allowing areas of fluid flow to form while the robot is in the environment. It was also noted that the results were better predicted in the near-wall force model in the following analysis. Fan et al. (2018) presented automatic microfluidic capturing using a magnetic micro-robot that resembles a peanut and exercising robotic manipulation. An electromagnetic actuator scheme is developed by using rolling and kayaking in the motion modes of the micro-robot. This research demonstrates the implementation of swimming microrobots in sub-micrometer dimensions. It is noted that said micro-robot can comfortably capture and manipulate a particle that is one hundred times bigger than itself. Steager et al. (2013) focused on the manipulation of cells and microbeads by magnetically powered micro-robots. These robotic manipulations, besides just moving the cell, present the creation and operation by outside magnetic fields of micron-sized biocompatible ferromagnetic micro-robot. The said microbeads in the article were automatically placed at the target location by creating localized magnetic gradients. Koens et al. (2019) reviewed the mechanisms with the help of the combination of theory and experimentation of the two micro rafts engaging with each other. Three models were merged to describe the dynamics of a new micro raft experiment by authors: mean division of rafts, mechanisms of disengagement of rafts, and configuration consolidation. Also, a broad array of capillary correlations between the disks identified for each pattern of arrangement. In a similar study, Li and Fukuda (2020) presented a study with the aim on the common point of engineering and art. Thanks to micro-robots that can be used in liquid media, magnetic guided manipulation is recommended to create designed patterns properly. The magnetically guided manipulation offers suggestions for practical scaffold development in tissue engineering, as well as a modern tool for drug distribution and gastrointestinal disease analysis in clinical research, and also offers a new methodology to non-invasive, non-destructive, and non-contact precision activity in biomedical engineering. However, micro-robots are placed methodically in the desired place to overcome the liquid disorder that may occur. Ye and Sitti (2014) focused on the capture of microorganisms in a liquid environment and their controlled transport in two dimensions. This approach aims to mitigate damage to biological samples otherwise inflicted by heat and light during manipulation. This technique presented in the paper was realized by a portable micro-robotic system to specifically capture and move specific microorganisms that float near to a planar solid surface at low Reynold numbers. The non-contact manipulation was achieved using local rotational fluid bubbles stimulated with fast-spinning spherical-shaped neodymium.

As can be seen in the literate, the method of non-contact manipulation by hydrodynamic interactions associated with induced flow fields has been studied extensively by theoretical and experimental means. Here, as stated earlier, the focus is on the simple but fast robotic model to predict the motion of a particle manipulated by the induced free vortex flow. The rigid body motion of the said particle is modeled via a novel approach based on Bernoulli's equation of conservation of energy across the streamlines, the free vortex flow field, and the implicit Magnus effect modeling on the captured particle. The particles are assumed to be of perfect spherical shape and the fluid drag on the particles is predicted via drag coefficients whereas the rigid-body accelerations of the particles are calculated under the influence of time-dependent magnetic and flow fields. The performance of the model is demonstrated by rigid-body acceleration, velocity, and displacement of the particles over time.

2. Numerical Modeling

Figure 1 illustrates two particles, one being rotated by the magnetic field while the other one is being captured and manipulated by the induced free vortex flow. The particle is passive and non-magnetic; thus, it is under the influence of the resultant flow field. The force balance is written in cylindrical coordinates. The non-magnetic particle is orbiting the magnetic particle that is being held in place and rotating at the core of the vortex by rotating the magnetic field. Both particles are assumed to be neutrally buoyant and submersed but far enough from any solid boundary to avoid additional drag (Higdon and Muldowney, 1995).

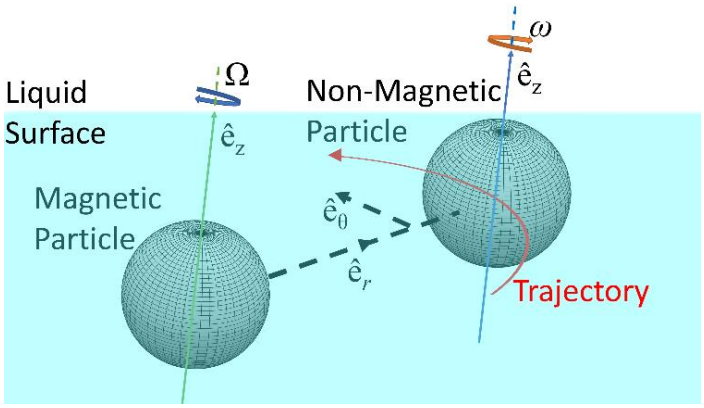

Figure 1: Magnetic particle and non-magnetic particle submerged in a large liquid bath. The magnetic particle being rotated by external magnetic field whereas the non-magnetic particle is under the influence of its flow, i.e., the free vortex. Rigid-body rotation axes and directions are chosen to agree with the model and simulation results.

The magnetic particle at the center is assumed to be rotating under the influence of a time-dependent magnetic field of adequate strength, i.e., $\mathbf{B} = [20\cdot\cos(2\pi\cdot f\cdot t)\ -20\cdot\cos(2\pi\cdot f\cdot t)\ 0]^T$ mT with a rotation rate of f = 5 Hz along the z-direction, for this study. The resultant flow field can be modeled using Bernoulli's conservation of energy equation across the streamlines. The flow field is assumed to be a free vortex. Using the two assumptions, it will be possible to predict the flow field in which the captured particle is being dragged. Thus, using the Bernouilli's equation, the pressure drop along the radial direction can be predicted and employed in the equation of motion. The radial force balance results in acceleration along r-axis whereas the azimuthal acceleration is observed due to viscous drag only. This model does not take capillary interaction between the magnetic particles and non-magnetic particle (Mastrangeli et al., 2010) nor it considers the added mass effect (Wang and Ardekani, 2012) in order to keep the focus on implications on the analysis based on Bernoulli's equation as described in this study.

The equation of motion for the magnetic particle rotating at the core is:

$$J\frac{d\Omega}{dt} = (\boldsymbol{m}\times\Re\boldsymbol{B}) - 8\pi\mu R^3\Omega. \quad (1)$$

Above, **m** stands for the magnetization vector of the magnetic body which is assumed to be spherical with the magnetic properties similar to that of a N52-grade Neodymium magnet (Dong et al., 2019) with the direction of $[1\ 0\ 0]^T$. Thus, the core of the vortex is rotating with the angular velocity of Ω rad/s under the influence of the applied magnetic field **B**. Here, J, μ, and R stand for the moment of inertia in kg·m^2, dynamic viscosity of the liquid in Pa·s, and radius of the magnetic particle at the vortex core in m. Furthermore, ℜ is the rotation matrix from the lab frame to the frame of the rotating magnetic particle.

The Bernoulli's equation for energy conservation across the streamlines is (Munson et al., 2005):

$$p - \rho\int\frac{v_\theta^2}{r}dr = \text{constant} \quad (2)$$

with p, ρ, v_θ, and r denoting static pressure in Pa, liquid density in kg/m^3, azimuthal velocity in rad/s, and radial position in m, respectively. The free vortex can be modeled as $v_\theta = \Gamma/(2\pi\cdot r)$ (Munson et al., 2005) with Γ being the circulation, i.e., $\Gamma = 2\pi\cdot\Omega\cdot R^2$, for the vortex-induced by the rotating core, i.e., the magnetic particle at the center. Furthermore, the captured non-magnetic material rotates along its axis of rotation along z-direction due to the torque owing to the net shear exerted on its surface that can be found by integrating infinitesimal shear-torque values along the z-axis, i.e., $dT = r\cdot\mu\cdot(dv_\theta/dr)\hat{e}_z$ N·m/m^2, over its entire surface. The resultant torque is found to be $T = 8\pi\cdot\mu\cdot R2\cdot\Omega\cdot a$ which is supposed to contribute to the relative velocity of the surface of the non-magnetic particle to the local flow field of the free vortex. Here, a signifies the radius of the non-magnetic particle. Thus, the equation of motion for the rigid-body rotation along the symmetry axis, with the moment of inertia of j, is given as:

$$j\frac{d\omega}{dt} = (-8\pi\mu R^2\Omega a - 8\pi\mu a^3\omega)\hat{e}_z. \quad (3)$$

This rotational velocity, ω rad/s, will be imposed on the surface on the non-magnetic particle based on the location with respect to the center of the vortex core, i.e., $\omega\cdot(r - r_p)$ m/s with r_p signifying the position of the non-magnetic particle with respect to the center of the vortex core. This correction in Bernoulli's equation will include the Magnus effect (Cipparrone et al., 2011) acting on the particle thus contributing to the equation of motion along the radial direction.

The drag force acting on an object moving with a speed U in an arbitrary direction $\hat{e}_i$ is given as $F_d = -\varsigma\cdot U\cdot\hat{e}_i$ (Berg, 1993). Here, ς denotes the linear drag coefficient, i.e., $\varsigma = -6\pi\cdot\mu\cdot a$. The drag force will be the main resistance to the rigid-body motion along the radial and azimuthal directions. Therefore, the equation of motion for the captured non-magnetic particle in the cylindrical coordinate system of the vortex core is then

$$m\frac{du_r}{dt} = \{-6\pi\mu a u_r - \pi a^2 \rho \int_{r_p-a}^{r_p+a} \frac{\left(\frac{\Omega R^2}{r} - \omega(r-r_p)\right)^2}{r} dr\}\hat{e}_r \quad (4)$$

along the radial direction, with u_r being the linear rigid-body velocity of the non-magnetic particle with respect to the center of the vortex core, and

$$m\frac{du_\theta}{dt} = -6\pi\mu a(u_\theta - v_\theta)\hat{e}_\theta \quad (5)$$

along the azimuthal direction with u_θ being the azimuthal rigid-body velocity of the non-magnetic particle captured by the local flow field. Here, m stands for the mass of the non-magnetic particle. The presence of Ω in all the equations of motion dictates that the system is coupled, resulting in the overall magnetohydrodynamic property for the system. This last equation of motion concludes the modeling for the described physical scenario under given assumptions.

3. Results and Discussion

The following results are obtained for two spherical particles identical in shape and dimensions and assumed to be naturally buoyant for sake of simplicity. The radius of the particles is 10 μm and the proximity is 40 μm. The liquid is water at room temperature. The simulation is carried out in Matlab/SIMULINK environment via time-integration over the rigid-body accelerations for a total of 10 seconds in real-time. The following plots are extracted directly from Simulink 'scope' block.

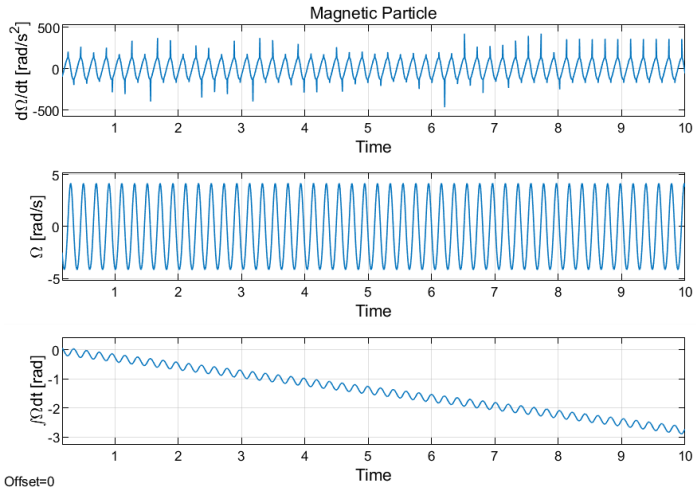

Figure 2: (Top) The angular acceleration, dΩ/dt, (Middle) the angular velocity, Ω, and (Bottom) the net rotation, ∫Ωdt, of the magnetic particle at the core of the free vortex, with respect to simulation time.

Figure 2 demonstrates the angular acceleration, velocity, and total rotation of the magnetic particle. It is observed that the magnetic field is rotating too fast for smooth time-dependent alignment between the magnetic field, **B,** and its magnetization vector, **m**. Therefore, the oscillation in velocity (Middle) is the well-known step-out phenomenon (Mahoney et al., 2014). The net rigid-body rotation (Bottom) is almost 3 rad in the clockwise direction in 10 seconds although the maximum instantaneous angular velocity is observed to be more than 4 rad/s. Also, the angular acceleration (Top) exhibits discontinuities due to a change in direction of rotation rate owing to the step-out phenomenon.

Figure 3 represents that the angular acceleration, velocity, and total rotation of the non-magnetic particle. The magnitude of the angular acceleration (Top) is found to be much larger than that of the magnetic particle depicted in Figure 2. The angular velocity (Middle) of the non-magnetic particle is directly related to the free vortex flow field which is subject to the step-out phenomena observed in Figure 2. The time-dependent and the net rigid-body revolution of the non-magnetic particle (Bottom) happens to be in a counter-clockwise direction; therefore, in the opposite direction of the revolution of the magnetic particle. Hence, the relative velocity on one side of the non-magnetic particle becomes zero maximizing the local pressure and opposing the pressure difference associated with the free vortex flow of the rotating magnetic particle.

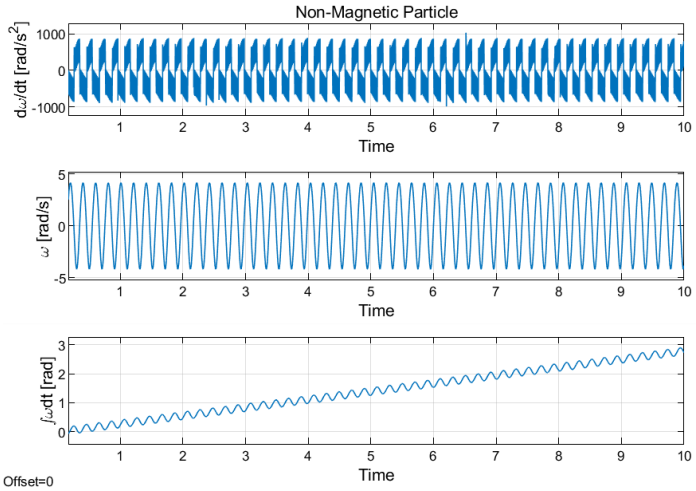

Figure 3: (Top) The angular acceleration, dω/dt, (Middle) the angular velocity, ω, and (Bottom) the net rotation, $\int\omega dt$, of the non-magnetic particle in the free vortex flow, with respect to simulation time.

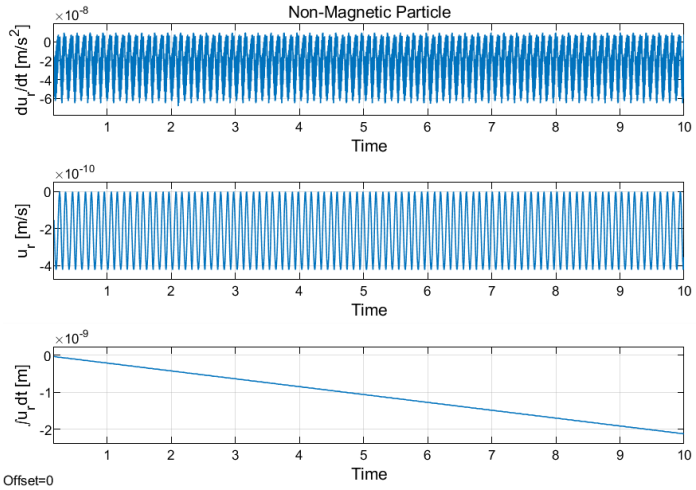

Figure 4: (Top) The radial rigid-body acceleration, du_r/dt, (Middle) the radial rigid-body velocity, u_r, and (Bottom) the net radial rigid-body displacement, $\int u_r dt$, of the non-magnetic particle at the core of the free vortex, with respect to simulation time.

Figure 4 depicts the rigid-body motion of the non-magnetic particle in the radial direction. It is very important to acknowledge that the order of net displacement in r-direction is

O(-9) as given in Figure 4 (Bottom). This behavior indicates a stable orbit around the vortex core and promising performance in controlled motion for the non-magnetic particle with frequency modulation of applied magnetic field, **B**. The rigid-body acceleration (Top) and velocity (Middle) are much smaller than the diameter of the particle. This also indicates that the pressure distribution on the surface of the non-magnetic particle is symmetric, i.e., the pressure difference due to free vortex flow field and the magnus effect cancel each other out. Therefore, infinitesimal pressure difference along the particle surface is the reason for the aforementioned performance of stable orbit.

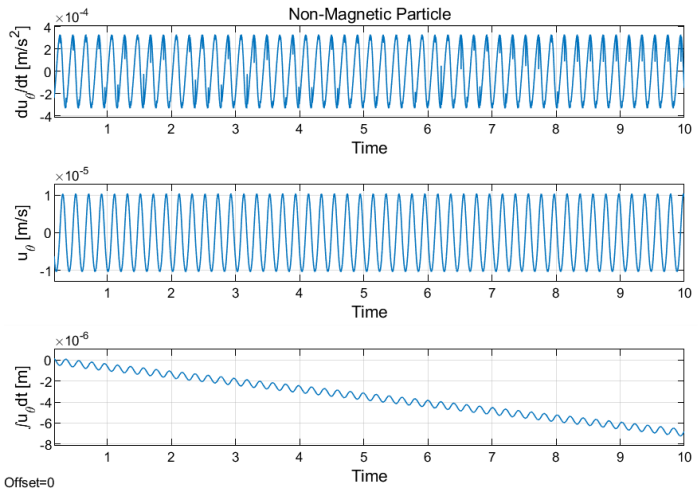

Figure 5: (Top) The azimuthal rigid-body acceleration, du_θ/dt, (Middle) the azimuthal rigid-body velocity, u_θ, and (Bottom) the net azimuthal rigid-body displacement, $\int u_\theta dt$, of the non-magnetic particle at the core of the free vortex, with respect to simulation time.

Figure 5 demonstrates the azimuthal rigid-body motion of the non-magnetic particle. The non-magnetic particle orbits around the free vortex core as expected with an oscillating velocity due to the step-out phenomenon, again. It has been observed that the particle completes a full orbit in less than 5 minutes (Bottom). The acceleration (Top) and the velocity (Middle) are comparable with the diameter of the particle. It is important to acknowledge that the force balance on the non-magnetic particle predicts steady periodic rigid-body acceleration and velocity with constant amplitude; thus, the model is well defined for the studied motion. Finally, with the help of the results observed via Figure 4 and 5, the Re number, i.e., $\mathrm{Re} = 2\rho Ua/\mu$ for the non-magnetic microparticle with which the term U is the magnitude of $[u_r\ u_\theta\ 0]^T$, is found to be on the order of *O*(-6) that emphasizes the fact that inertia is dominated by the shear within the flow fields, thus the drag coefficient approach to find the fluid forces exerted on the micro particles is numerically validated.

4. Conclusions and Recommendations

The robotic model based on Bernoulli's conservation of energy across the streamlines for curvilinear motion along the flow field induced by free vortex seems to predict stable orbit without capillary forces and added mass effects. However, capillary forces will be important for particles floating on the liquid surface with a certain contact angle. Furthermore, with the contact angle, the liquid surface is expected to have a curved profile. Furthermore, along the surface, it is possible to observe interfacial vibrations (Ergin et al., 2017). However, in this study the particles are assumed to be neutrally buoyant and fully submerged for sake of simplicity. The model can be used for design of experiments, optimization, and control of non-contact micromanipulation in biomedical micro-robotic applications. The model provided here might be validated with the experimental results in the literature after the interfacial effects and the boundary effects are properly incorporated in the equations of motion. Finally, the analysis should be carried out for particles of arbitrary shapes, denoting cells, to obtain more useful insight for real biomedical applications.

References

Zhang, Z., Wang, X., Liu, J., Dai, C., & Sun, Y. (2019). Robotic Micromanipulation: Fundamentals and Applications. *Annual Review of Control, Robotics, and Autonomous Systems*, *2*(1), 181–203. https://doi.org/10.1146/annurev-control-053018-023755

Diller, E., Ye, Z., Giltinan, J., & Sitti, M. (2014). Addressing of Micro-robot Teams and Non-contact Micro-manipulation. *Small-Scale Robotics. From Nano-to-Millimeter-Sized Robotic Systems and Applications*, 28–38. https://doi.org/10.1007/978-3-642-55134-5_3

Zhang, Y., Lin, S., Liu, Z., Zhang, Y., Zhang, J., Yang, J., & Yuan, L. (2020). Laser-induced rotary micromotor with high energy conversion efficiency. *Photonics Research*, *8*(4), 534. https://doi.org/10.1364/prj.381397

Mohanty, S., Khalil, I. S. M., & Misra, S. (2020). Contactless acoustic micro/nano manipulation: a paradigm for next generation applications in life sciences. *Proceedings of the Royal Society A: Mathematical, Physical and Engineering Sciences*, *476*(2243), 20200621. https://doi.org/10.1098/rspa.2020.0621

Diller, E., Ye, Z., & Sitti, M. (2011, September). Rotating magnetic micro-robots for versatile non-contact fluidic manipulation of micro-objects. *2011 IEEE/RSJ International Conference on Intelligent Robots and Systems*. https://doi.org/10.1109/iros.2011.6094968

Ye, Z., Diller, E., & Sitti, M. (2012). Micro-manipulation using rotational fluid flows induced by remote magnetic micro-manipulators. *Journal of Applied Physics*, *112*(6), 064912. https://doi.org/10.1063/1.4754521

Pieters, R. S., Tung, H.-W., Sargent, D. F., & Nelson, B. J. (2014). Non-contact Manipulation for Automated Protein Crystal Harvesting using a Rolling Microrobot. *IFAC Proceedings Volumes*, *47*(3), 7480–7485. https://doi.org/10.3182/20140824-6-za-1003.00398

Zhang, S., Scott, E. Y., Singh, J., Chen, Y., Zhang, Y., Elsayed, M., Chamberlain, M. D., Shakiba, N., Adams, K., Yu, S., Morshead, C. M., Zandstra, P. W., & Wheeler, A. R. (2019). The optoelectronic microrobot: A versatile toolbox for micromanipulation. *Proceedings of the National Academy of Sciences*, *116*(30), 14823–14828. https://doi.org/10.1073/pnas.1903406116

Floyd, S., Pawashe, C., & Sitti, M. (2009). Two-Dimensional Contact and Noncontact Micromanipulation in Liquid Using an Untethered Mobile Magnetic Microrobot. *IEEE Transactions on Robotics*, *25*(6), 1332–1342. https://doi.org/10.1109/tro.2009.2028761

Fan, X., Sun, M., Lin, Z., Song, J., He, Q., Sun, L., & Xie, H. (2018). Automated Noncontact Micromanipulation Using Magnetic Swimming Microrobots. *IEEE Transactions on Nanotechnology*, *17*(4), 666–669. https://doi.org/10.1109/tnano.2018.2797325

Steager, E. B., Selman Sakar, M., Magee, C., Kennedy, M., Cowley, A., & Kumar, V. (2013). Automated biomanipulation of single cells using magnetic microrobots. *The International Journal of Robotics Research*, *32*(3), 346–359. https://doi.org/10.1177/0278364912472381

Koens, L., Wang, W., Sitti, M., & Lauga, E. (2019). The near and far of a pair of magnetic capillary disks. *Soft Matter*, *15*(7), 1497–1507. https://doi.org/10.1039/c8sm02215a

Li, X., & Fukuda, T. (2020). Magnetically Guided Micromanipulation of Magnetic Microrobots for Accurate Creation of Artistic Patterns in Liquid Environment. *Micromachines*, *11*(7), 697. https://doi.org/10.3390/mi11070697

Ye, Z., & Sitti, M. (2014). Dynamic trapping and two-dimensional transport of swimming microorganisms using a rotating magnetic microrobot. *Lab Chip*, *14*(13), 2177–2182. https://doi.org/10.1039/c4lc00004h

Higdon, J. J. L., & Muldowney, G. P. (1995). Resistance functions for spherical particles, droplets and bubbles in cylindrical tubes. *Journal of Fluid Mechanics*, *298*, 193–210. https://doi.org/10.1017/s0022112095003272

Mastrangeli, M., Valsamis, J.-B., Van Hoof, C., Celis, J.-P., & Lambert, P. (2010). Lateral capillary forces of cylindrical fluid menisci: a comprehensive quasi-static study. *Journal of Micromechanics and Microengineering*, *20*(7), 075041. https://doi.org/10.1088/0960-1317/20/7/075041

Wang, S., & Ardekani, A. M. (2012). Unsteady swimming of small organisms. *Journal of Fluid Mechanics*, *702*, 286–297. https://doi.org/10.1017/jfm.2012.177

Dong, F., Huang, Z., Qiu, D., Hao, L., Wu, W., & Jin, Z. (2019). Design and Analysis of a Small-Scale Linear Propulsion System for Maglev Applications (1)—The Overall Design Process. *IEEE Transactions on Applied Superconductivity*, *29*(2), 1–5. https://doi.org/10.1109/tasc.2019.2895337

Munson, B. R., Young, D. F., & Okiishi, T. H. (2005). *Fundamentals of Fluid Mechanics* (5th ed.). Wiley.

Cipparrone, G., Hernandez, R. J., Pagliusi, P., & Provenzano, C. (2011). Magnus force effect in optical manipulation. *Physical Review A*, *84*(1), 015802. https://doi.org/10.1103/physreva.84.015802

Berg, H. C. (1993). *Random Walks in Biology: New and Expanded Edition* (Revised ed.). Princeton University Press.

Mahoney, A. W., Nelson, N. D., Peyer, K. E., Nelson, B. J., & Abbott, J. J. (2014). Behavior of rotating magnetic microrobots above the step-out frequency with application to control of multi-microrobot systems. *Applied Physics Letters*, *104*(14), 144101. https://doi.org/10.1063/1.4870768

Ergin, F. G., Tabak, A. F., Wang, W., & Sitti, M. (2017, June). Time-resolved measurements of the free surface motion due to spinning micro-rafts using Stereo MicroPIV. Www.Dantecdynamics.Com. https://www.dantecdynamics.com/wp-content/uploads/2019/11/time-resolved_measurements_of_the_free_surface_motion_due_to_spinning_micro-rafts_using_stereo_micropiv-1.pdf